

RESEARCH

Open Access



Arachidonic acid is involved in high-salt diet-induced coronary remodeling through stimulation of the IRE1 α /XBP1s/RUNX2/OPN signaling cascade

Zhuoran Jia¹, Jian Wu¹, Fang Liu¹, Huimin Wang¹, Peiyang Zheng¹, Bing Shen² and Ren Zhao^{1*}

Abstract

Background The impact of a high-salt (HS) diet on metabolic disturbances in individuals with coronary heart disease remains unclear. The arachidonic acid (AA) metabolic pathway is closely linked to the development of cardiometabolic diseases and atherosclerotic cardiovascular diseases. Furthermore, endoplasmic reticulum stress (ERS) has emerged as a major contributor to cardiometabolic diseases. AA-related inflammation and ERS are hypothesized to play a role in HS diet-induced coronary remodeling.

Methods Rats were subjected to an HS diet for 4 weeks, and the serum concentration of AA was measured via enzyme-linked immunosorbent assay. Immunofluorescence staining and vascular tension measurements were conducted on coronary arteries. In addition, AA-stimulated coronary artery smooth muscle cells (CASMCs) were treated with ERS inhibitors to explore the underlying pathway involved.

Results Increased susceptibility to myocardial infarction in the HS diet-fed rats was accompanied by increased serum AA concentrations and increased expression of the key AA metabolic enzyme cyclooxygenase-2 (COX-2). AA incubation weakened the contraction of denuded coronary arteries, reduced the expression of contraction markers, and increased the fluorescence intensity of synthetic and ERS response markers in coronary arteries. Further investigation of CASMCs revealed that AA-induced phenotypic transformation was mediated via the ERS pathway.

Conclusions ERS and AA were found to be stimulated in CASMCs following an HS diet. AA triggers an ERS response through COX-2 catalysis, and the downstream inositol requiring enzyme 1 - X-box binding protein-1 - osteopontin pathway may contribute to the AA-induced phenotypic transformation of CASMCs, resulting in dysfunctional coronary tension. This study may provide potential therapeutic targets for cardiovascular diseases associated with excessive AA-derived ERS.

Keywords Arachidonic acid, High-salt diet, Coronary artery smooth muscle cells, Endoplasmic reticulum stress, Osteopontin, Phenotypic transformation

*Correspondence:
Ren Zhao
zhaoren@ahmu.edu.cn

¹Department of Cardiology, The First Affiliated Hospital of Anhui Medical University, 218 Jixi Road, Hefei 230022, Anhui, China
²Department of Physiology, School of Basic Medical Sciences, Anhui Medical University, Hefei 230032, Anhui, China



© The Author(s) 2025. **Open Access** This article is licensed under a Creative Commons Attribution-NonCommercial-NoDerivatives 4.0 International License, which permits any non-commercial use, sharing, distribution and reproduction in any medium or format, as long as you give appropriate credit to the original author(s) and the source, provide a link to the Creative Commons licence, and indicate if you modified the licensed material. You do not have permission under this licence to share adapted material derived from this article or parts of it. The images or other third party material in this article are included in the article's Creative Commons licence, unless indicated otherwise in a credit line to the material. If material is not included in the article's Creative Commons licence and your intended use is not permitted by statutory regulation or exceeds the permitted use, you will need to obtain permission directly from the copyright holder. To view a copy of this licence, visit <http://creativecommons.org/licenses/by-nc-nd/4.0/>.

Background

Cardiometabolic (CM) diseases pose a major global public-health challenge, with chronic inflammation being a key underlying pathological process. Factors such as a high-salt diet, diabetes, stroke, and chronic coronary heart disease contribute to this inflammatory process [1]. Recent studies have revealed that high salt intake not only increases blood pressure but also independently promotes coronary vascular remodeling. New research has shown that high salt (HS; NaCl) content in food can alter immune function, leading to a shift toward a proinflammatory state. Arachidonic acid (AA), a type of polyunsaturated fatty acid, plays an essential role in many physiological functions, such as growth, reproduction, stress resistance, immunity, lipid deposition, and bone development [2]. AA is metabolized via several enzymes and participates in numerous metabolic pathways. Pathways mediated by AA have been associated with the development of cardiovascular ischemia-reperfusion injury [3] and cerebral infarction [4]. Cyclooxygenase-2 (COX-2), a key enzyme responsible for converting AA into prostaglandin E2 (PGE2), is notably upregulated in atherosclerotic plaques and aortic aneurysms in both human tissues and animal models [5]. The AA-COX-2 pathway primarily contributes to the inflammatory process [6]. However, the precise mechanisms through which the AA-COX-2 pathway influences coronary smooth muscle cells (CASCs) and their associated molecular signaling remain unclear.

In healthy blood vessels, vascular smooth muscle cells (VSMCs) typically maintain a contractile morphology. However, when blood vessels suffer damage or are influenced by pathological factors, VSMCs can change their phenotype, shifting from a contractile state to one that is proliferative and synthetic [7]. During this change, the expression level of a specific contraction marker called α -smooth muscle actin (α -SMA) decreases, whereas the expression of a synthetic marker known as osteopontin (OPN) increases [8]. This transformation is implicated in the development of many vascular disorders, such as hypertension [9], atherosclerosis [10], pulmonary hypertension [11], and postoperative restenosis [12]. The phenotypic transformation of VSMCs is intricately connected to biological processes such as immunoinflammatory responses, oxidative stress, and vascular remodeling [13]. Previous research has suggested that AA metabolism not only regulates platelet aggregation [14] but also contributes to the phenotypic transformation of CASCs.

The endoplasmic reticulum (ER) is a versatile organelle, with various functions, including protein synthesis, folding, transport, calcium homeostasis regulation, and lipid biosynthesis [15]. Pathological factors such as oxidative stress, ischemia, hypoxia, and disturbances in

calcium homeostasis can lead to the buildup of misfolded or unfolded proteins in the ER, triggering endoplasmic reticulum stress (ERS) [15]. Inositol-requiring enzyme 1 (IRE1), a transmembrane protein found on the membrane of the endoplasmic reticulum, detects endoplasmic reticulum stress (ERS). Under normal conditions, IRE1 associates with glucose-regulated protein 78/binding immunoglobulin protein (GRP78/BiP). However, during ERS, unfolded or misfolded proteins recruit GRP78, causing its dissociation from IRE1. Activated IRE1 then acts on X-box binding protein-1 (XBP1) mRNA, excising a 26-nucleotide intron and changing its coding reading frame. This process results in the generation of XBP1s, which is a more stable form of the protein. XBP1s increases the capacity of the ER to fold proteins [10]. Research has shown that the IRE1-XBP1s signaling pathway, a key component of the ERS response, plays a role in promoting the survival and proliferation of VSMCs [12], and ERS has been implicated in liver injury through the IRE1-XBP1s pathway in hepatocytes [13]. However, whether the ERS response and its downstream IRE1-XBP1s signaling pathways are involved in AA-mediated phenotypic transformation has not been reported. The phenotypic transformation of VSMCs is a critical early stage in the development of cardiovascular diseases. If the ERS response is indeed involved in the pathological mechanism of the phenotypic transformation of VSMCs, the ER may be a promising new target for drugs aimed at preventing or treating cardiovascular conditions.

Some evidence suggests a link between AA and ERS. The AA-cytochrome P450 (CYP450) pathway can induce an ERS response in hepatocytes [16]. Additionally, when cells are exposed to harmful stimuli, COX-2 converts AA to PGE2. Inhibitors of PGE2 alleviate ERS-mediated apoptosis in osteoarthritis [17]. However, whether AA induces an ERS response in CASCs through the COX-2 pathway remains unknown. Consequently, further research is necessary to explore the mechanism of AA and ERS damage in CASCs and its impact on coronary artery tension. On the basis of this hypothesis, this study proposes that the AA metabolic pathway promotes the phenotypic transformation of CASCs and contributes to coronary artery tension injury through the ERS signaling pathway.

This research investigated the roles of AA and ERS in vascular remodeling induced by a HS diet. This study specifically demonstrated that AA promotes the phenotypic transformation of vascular smooth muscle by increasing ERS activity, particularly through the IRE1-XBP1s signaling pathway—a novel discovery that has not been previously documented. These findings suggest that targeting ERS could be a promising approach for treating vascular remodeling diseases.

Methods

Materials

AA was sourced from Abcam (ab120916) and prepared in dimethyl sulfoxide (DMSO). The ERS inhibitor 4-phenylbutyric acid (4-PBA), acquired from Med Chem Express, was also dissolved in DMSO. NS-398, a COX-2 inhibitor, was procured from Sigma and similarly dissolved in DMSO. The primary rabbit antibody targeting p-IRE1 α (ab124945) was supplied by Abcam. The primary rabbit antibodies against COX-2 (12375-1-AP), XBP1s (24868-1) and runt-related transcription factor 2 (RUNX2) (20700-1) were acquired from Proteintech Biotechnology. Primary antibodies against OPN (mouse, sc-21742) and IRE1 α (mouse, sc-390960) were obtained from Santa Cruz Biotechnology. Primary rabbit antibodies against α -SMA (AF1032) and GRP-78 (AF5366) were obtained from Affinity. The secondary antibodies utilized included donkey anti-mouse IgG (H+L), which is highly cross-adsorbed and conjugated with Alexa Fluor 488 (A21202), as well as donkey anti-rabbit IgG (H+L), which is highly cross-adsorbed and conjugated with Alexa Fluor 555 (A31572). Both antibodies were obtained from Thermo Fisher Scientific.

Animal preparation

Adult male SD rats (180 g, 6 weeks old) were randomly assigned to two separate groups. The control group received a standard diet containing 0.4% sodium chloride, whereas the HS diet group was given food with 8% NaCl and was maintained in a vivarium with controlled temperature and humidity. These diets were administered to the rats for a duration of 4 weeks. The vivarium followed a cycle of 12 h of light followed by 12 h of darkness, and the rats had unrestricted access to food and water. All the animal studies were conducted following the National Institutes of Health guidelines (publication No. 8523) and received approval from the Animal Experimentation Ethics Committee at Anhui Medical University (Anhui Medical Ethics Approval No. LLSC20190530).

Cell preparation and culture

The rats were humanely euthanized by an overdose of CO₂. Coronary artery smooth muscle cells (CASMCs) were isolated following the protocol described in a previous study [18]. Briefly, the coronary artery was carefully dissected in a sterile environment and placed in sterile phosphate-buffered saline (PBS). Under a microscope, the arterial cavity was longitudinally incised, and the endothelial layer was mechanically removed via a sterile cotton swab. Smooth muscle tissue from the adventitia was separated. The isolated tissue was then cultured in a mixture containing 0.2% type 1 A collagenase, 0.9% papain, 0.5% bovine serum albumin (BSA), and Ca²⁺-free PBS at 37 °C for 50 min. After this incubation period,

the CASMCs were dispersed and gently washed with PBS before being transferred to a new dish. These cells were then grown in Dulbecco's modified Eagle's medium (DMEM) enriched with 20% fetal bovine serum, 100 μ g/ml penicillin, and 100 U/ml streptomycin. CASMCs were allowed to grow for 5–7 days prior to the start of the experiment.

Dosage information

Myocardial ischemia was induced in male rats via subcutaneous isoproterenol (ISO) injection (85 mg/kg body weight) on the 29th and 30th days. For the vascular tension experiment, the coronary arteries were incubated with 10 μ M AA for 24 h. CASMCs were subjected to incubation with various concentrations of AA (1, 3, 10, 30, or 100 μ M) for different durations (0, 12, 24, 36, or 48 h). The optimal concentration and time for AA treatment were subsequently determined to be 10 μ M and 24 h, respectively. For subsequent experiments involving CASMCs to investigate this pathway, the cells were treated concurrently with 10 μ M AA and 1 mM ERS inhibitor (4-PBA) for 24 h. Similarly, CASMCs were treated with 10 μ M AA and 10 mM COX-2 inhibitor (NS-398) simultaneously for 24 h.

Electrocardiogram (ECG) recording

ECG recordings were performed on the rats on the 1st, 28th and 30th days to assess the state of myocardial ischemia. The rats received an intraperitoneal pentobarbital sodium injection (50 mg/kg) to ensure immobilization while maintaining spontaneous breathing. The electrodes were placed subcutaneously in a standard limb lead configuration (Lead II). ECG signals were recorded via a data acquisition system (BL-420 S, TECHMAN). The entire procedure was conducted under controlled ambient temperature (22–25 °C) to prevent external influences on cardiac function.

Triphenyltetrazolium chloride (TTC) staining

After the ECG measurements were completed, the rats were euthanized by an overdose of anesthesia, and the hearts were immediately excised and washed in ice-cold saline to remove blood. The hearts were then frozen briefly at –20 °C for 10 min to facilitate sectioning. Transverse slices of 1–2 mm thickness were obtained from the heart and incubated in 1% TTC solution at 37 °C for 20 min in the dark. TTC selectively stains viable myocardium red, whereas infarcted tissue remains pale or white. After staining, the slices were photographed.

ELISA

For measurement of the serum concentration of AA in the rats, each sample was diluted in PBS at an optimal ratio for analysis. The measurement was conducted using

a commercial ELISA kit (No. D751021, Sangon Biotech), following the provided instructions. A standard curve was generated using linear regression via OriginPro software (version 8.0, OriginLab) to determine the levels of AA.

Immunofluorescence

For coronary artery tissue, rat hearts were harvested after euthanasia, and coronary arteries were carefully dissected. The tissue samples were cryopreserved in OCT compound. Cryosections (7 μm thick) were obtained and mounted on glass slides suitable for immunofluorescence staining. After PBS washes, 0.1% Triton X-100 was used to permeabilize the tissue. Then, the tissue was preincubated with 3% BSA, followed by overnight incubation at 4 °C with primary antibodies against OPN, COX-2, IRE1 α , p-IRE1 α , XBP1s, RUNX2, and GRP-78 (dilution: 1:200). After thorough rinsing with PBS, the tissue sections were treated with secondary antibodies (anti-rabbit, 555 nm, red fluorescence, anti-mouse, 488 nm, and green fluorescence; Thermo Fisher Scientific) (dilution: 1:1000) for 1 h at 37 °C. Counterstaining with 4',6-diamidino-2-phenylindole (DAPI) facilitated nuclear visualization. For CASMC experiments, CASMCs were seeded in 12-well plates containing cover glass slides. When the cells reached a confluency of 70–80%, they were fixed using 4% paraformaldehyde for 20 min, followed by rinsing with PBS. A 0.1% Triton X-100 solution was applied and left at room temperature for 15 min to permeabilize the cell membranes. Subsequently, the CASMCs were treated with a 3% BSA solution to prevent nonspecific binding, incubating for one hour at room temperature. They were then allowed to incubate overnight with the primary antibody at 4 °C. Following this incubation, the cells underwent three five-minute washes with PBS. The samples were subsequently treated with a donkey anti-mouse IgG conjugated to Alexa Fluor 488, diluted at 1:1000, for two hours at room temperature. Once the secondary antibody was removed, the cells were washed three more times with PBS, each lasting five minutes. Nuclear staining was performed via incubation with DAPI for 5 min, followed by three additional washes with PBS for 5 min each. The fluorescence signals were captured, images were obtained utilizing a laser scanning microscope (Olympus, Japan), and ImageJ software (National Institutes of Health, NIH) was used for image analysis.

Cell proliferation assay

To gauge the proliferation capacity of CASMCs, a Cell Counting Kit-8 (CCK-8) assay (C0038, Beyotime) was employed. In short, CASMCs were seeded into 96-well plates and left to settle overnight. Once the cells had firmly attached, they were exposed to either 3 μM AA, 10

μM AA, or a vehicle control (CON) for a 24-hour period at 37 °C in a 5% CO₂ environment. Post-incubation, 10 μL of CCK-8 solution was introduced into each well, and the plates were incubated for an additional hour at 37 °C. Finally, the absorbance was measured at 450 nm using a microplate reader. The optical density (OD) readings were documented and adjusted to reflect the values of the control group. The summarized OD data for CASMCs exposed to CON, 3 μM AA, or 10 μM AA are displayed as the mean \pm standard error of the mean (SEM).

Vessel tension measurement

Measurements of vessel tension were performed following the methodology outlined in a previous publication [19]. Coronary arteries from healthy control rats, after the rats were euthanized, the coronary arteries were promptly dissected and immersed in Krebs Henseleit solution containing the following concentrations (in mmol/L): NaCl, 118; KCl, 4.7; KH₂PO₄, 1.2; CaCl₂, 2.5; NaHCO₃, 25.2; glucose, 11.1; and MgSO₄ (7 H₂O), 1.2. Microscopic examination entailed delicately rubbing the luminal surface of the arteries to carefully remove the endothelial layer. The vessels were then sliced into rings approximately 2 mm in length. Isometric tension was measured and analyzed using a DMT myograph (Model 610 M; Danish Myo Technology, Aarhus, Denmark), with the baseline tension established at 2.0 mN. Once the vessel tension stabilized, the Krebs–Henseleit solution was replaced with a 60 mmol/L K⁺ solution, which served as the reference contraction stimulus. For analysis of the activity of the coronary artery endothelium, 3 μM 9,11-dideoxy-11 α ,9 α -epoxymethanoprostaglandin (U46619) was used to induce contraction in the coronary artery rings for 5 min. Subsequently, 5 μM acetylcholine (ACh), a well-known endothelium-dependent vasodilator, was administered. A vasodilatory response to ACh below 20% of U46619-induced maximum contraction confirmed successful endothelial removal. Following this step, the vessels were thoroughly washed to restore baseline tension. Subsequently, U46619 (0.01–1 μM) and CaCl₂ (1–10 mM) were sequentially utilized to induce concentration-dependent contractions in the blood vessels.

Western blotting

Proteins were removed from coronary tissue and CASMCs using a detergent extraction buffer. The buffer composition included 150 mM NaCl, 20 mM Tris-HCl (pH 7.5), 1% NP-40, 0.1% sodium dodecyl sulfate, 0.5% sodium deoxycholate, 2.5 mM sodium pyrophosphate and 1 mM disodium salt of ethylenediaminetetraacetic acid, along with protease inhibitor cocktail tablets. A total of 20 μg of total protein from tissue homogenate or cell lysate was loaded into the wells of an SDS-gel, along

with a molecular weight marker. The proteins were then separated on 10% SDS-polyacrylamide gels and subsequently transferred to polyvinylidene difluoride membranes. Following blocking, the membranes were then incubated with primary antibodies at specific dilutions: anti-OPN (1:500), anti- α -SMA (1:500), anti-COX-2 (1:1000), anti-IRE1 α (1:500), anti-p-IRE1 α (1:500), anti-XBP1s (1:500), anti-RUNX2 (1:500), anti-GRP78 (1:500), or anti-GAPDH (1:1000), overnight at 4 °C. Following this, the membranes were treated with a horseradish peroxidase-conjugated secondary antibody and visualized using an enhanced chemiluminescence detection kit. Protein band intensities were quantified using ImageJ software, with each blot's optical density normalized to the corresponding GAPDH band in the same lane. The results were expressed as relative optical density values.

Statistics

The data are presented as the mean \pm SEM. Statistical charts were generated via GraphPad Prism software (GraphPad Software, USA). Statistical significance was assessed via either two-way ANOVA or a t-test. The results were considered significant when $P < 0.05$. The value of n represents the number of experiments conducted.

Results

A high-salt diet induces myocardial ischemia accompanied by elevated arachidonic acid levels

The HS diet is one of the primary risk factors for cardiac metabolic diseases and is associated with increased mortality in cardiovascular diseases. The rats were randomly divided into two groups: a normal control (NC) group and a high-salt (HS) group (Fig. 1A). The NC group

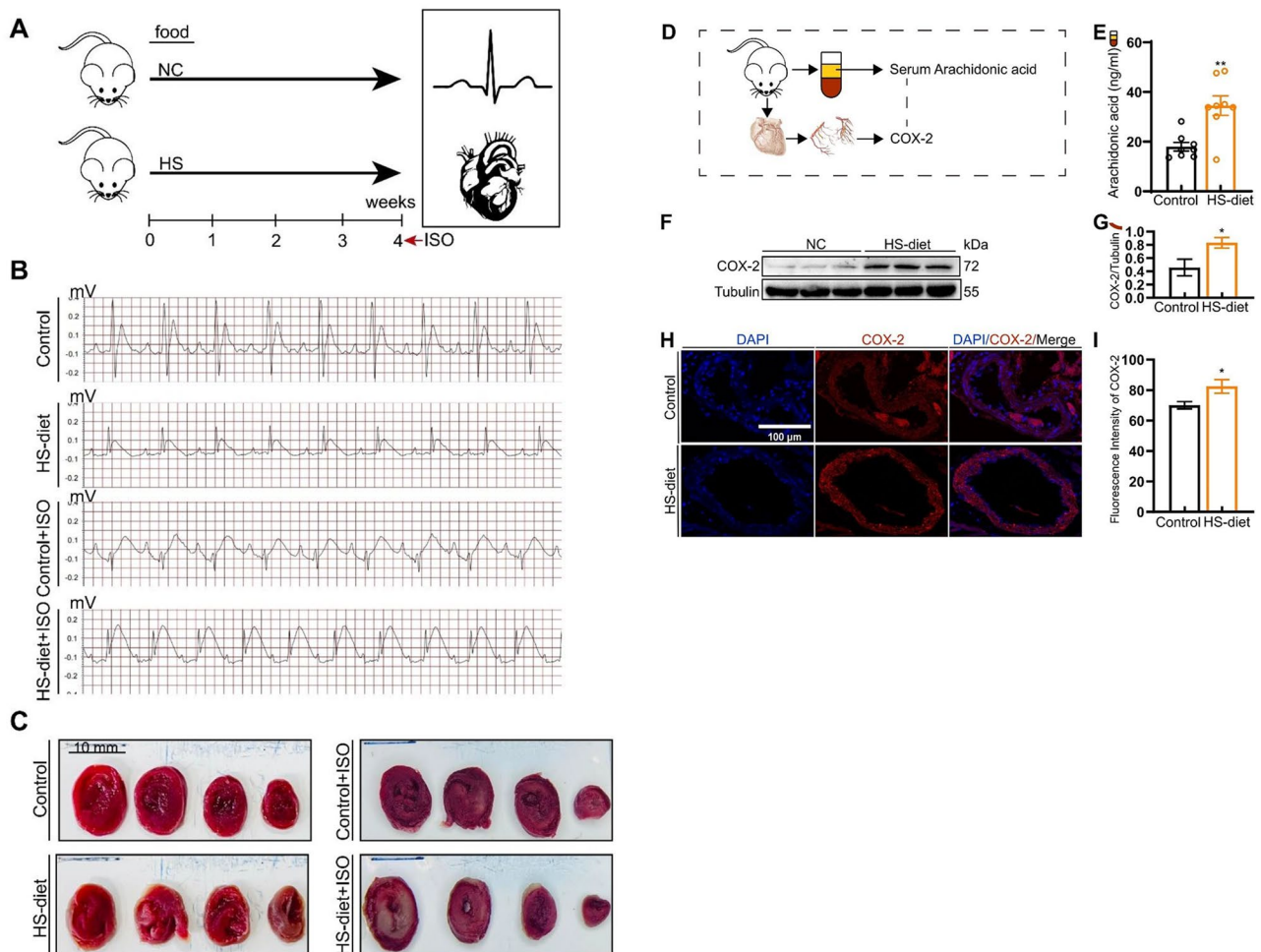


Fig. 1 A high-salt diet induces myocardial ischemia accompanied by elevated arachidonic acid levels. **(A)** Construction of the animal model. **(B)** Results of the rat electrocardiogram ($n=4$). **(C)** TTC staining results of rat hearts ($n=4$). **(D)** Experimental design, including measurement of serum AA levels and COX-2 protein expression in coronary arteries. **(E)** Serum AA levels in the rats ($n=8$). **(F)** Western blot analysis of COX-2 protein expression in coronary arteries and **(G)** analysis of band density ($n=3$). **(H)** Immunofluorescence detection of COX-2 expression in coronary arteries and **(I)** analysis of fluorescence intensity ($n=4$). The data are presented as the means \pm SEMs, * $P < 0.05$, ** $P < 0.01$, compared with the data of the control group. Abbreviations: TTC, triphenyltetrazolium chloride; AA, arachidonic acid; COX-2, cyclooxygenase-2

consumed a 0.4% sodium chloride diet, while the HS group was provided an 8% sodium chloride diet for four weeks. ECGs were recorded on Days 1 and 28. On Days 29 and 30, the rats underwent subcutaneous injections of ISO to induce myocardial infarction, with the control group receiving equivalent volumes of physiological saline. ECGs were recorded again on Day 30, after which the hearts were excised and stained with TTC to assess myocardial infarction. The ECG results (Fig. 1B) revealed that the control group maintained sinus rhythm without pathological T wave changes, whereas the HS-diet group also exhibited sinus rhythm but with ST-T changes, indicating myocardial ischemia. After ISO injection, both groups presented sinus rhythm, abnormal Q waves, ST-segment elevation, and increased T-wave amplitude, which was consistent with myocardial infarction. TTC staining (Fig. 1C) revealed that in the absence of ISO, the myocardial tissues in both groups were uniformly red, indicating viable myocardium without evident infarction. However, after ISO injection, the HS-diet group presented significantly larger pale areas than the normal diet group did, indicating more extensive tissue infarction. HS is a risk factor for cardiovascular injury, potentially involving impairments in coronary vasomotor function. Unsaturated fatty acids, particularly AA, are closely linked to heart metabolic diseases [20]. However, the relationship between the concentration of AA in vivo and the HS diet remains unclear. In this study, serum samples were collected from rats fed HS and normal diets to determine the concentration of AA and assess the expression of its key metabolic enzymes (Fig. 1D). The results revealed that the serum concentration of AA in the HS diet-fed group was greater than that in the control group (Fig. 1E). Subsequently, western blotting and immunofluorescence were employed to assess the expression levels of COX-2, a pivotal enzyme in arachidonic acid metabolism, in the coronary arteries of the HS diet group and the control group. The western blot results (Fig. 1F&G) indicated that, compared with that in the control group, the expression of COX-2 was elevated in the coronary arteries of the HS diet group. Similarly, immunofluorescence analysis (Fig. 1H&I) revealed an increase in COX-2 protein expression in the coronary arteries of the HS diet group compared with those of the control group. On the basis of these findings, it can be inferred that an HS diet increases serum AA levels and susceptibility to myocardial infarction.

A high-salt diet increases arachidonic acid levels, triggering coronary artery remodeling

Vascular remodeling is a common occurrence in hypertension, atherosclerosis, and other cardiovascular diseases. One important aspect of vascular remodeling is the phenotypic switch of smooth muscle cells, wherein

they transition from a contractile to a proliferative state. This transition is characterized by increased synthesis of the osteopontin protein and reduced expression of the α -SMA protein [21]. Specific fluorescent antibodies against the α -SMA and OPN proteins were used to label tissue sections from the coronary arteries of the rats to investigate whether coronary artery remodeling occurred in those fed an HS diet. The immunofluorescence results indicated that, in the HS diet-fed rats, the fluorescence intensity of α -SMA in the coronary arteries was significantly lower than that in the control group, whereas the fluorescence intensity of OPN was notably greater (Fig. 2A-D). This finding suggests a phenotypic change from contractile to proliferative in the coronary arteries. The increased proliferative capacity of CASMCs upon incubation with AA further supports these findings (Fig. 2E). To determine whether AA can influence this phenotypic switch in smooth muscle cells, CASMCs were pretreated with different concentrations (0, 3, 10, 30, or 100 μ M) of AA for 24 h. AA promoted CASMC phenotypic switching in a dose-dependent manner, with a reduction in α -SMA levels and an increase in OPN expression observed starting with 10 μ M AA incubation (Fig. 2F-H). Additionally, exposure to 10 μ M AA for varying time periods (0, 12, 24, 36, and 48 h) further promoted CASMC phenotypic alterations, as shown by increased synthesis of the CASMC synthetic protein OPN and decreased expression of the CASMC contractile protein α -SMA (Fig. 2I-K). These results indicate a close association between HS diet-induced coronary artery remodeling and AA.

Involvement of endoplasmic reticulum stress-related phenotypic changes in CASMCs following a high-salt diet

During ERS, folded or misfolded proteins recruit GRP78 while separating from IRE1 to form p-IRE1. X-box binding protein 1 (XBP1), a crucial transcription factor controlling the ERS response, is cleaved by the activated endoribonuclease domain of IRE1, resulting in the spliced active transcription factor XBP1s, which is crucial for maintaining ER homeostasis. Thus, XBP1s expression increases during ERS. To investigate the potential relationship between HS diet-induced coronary phenotypic transformation and ERS, the expression of ERS-related signaling proteins (IRE1 α , XBP1, and GRP78) in coronary arteries between the HS diet group and the control group was compared via immunofluorescence (Fig. 3A-C). An increase in the expression of these ERS-related proteins in the coronary arteries of HS diet-fed rats was observed (Fig. 3D-F). These findings led us to speculate that ERS may be involved in the AA-induced phenotypic transformation of CASMCs and subsequent coronary artery remodeling.

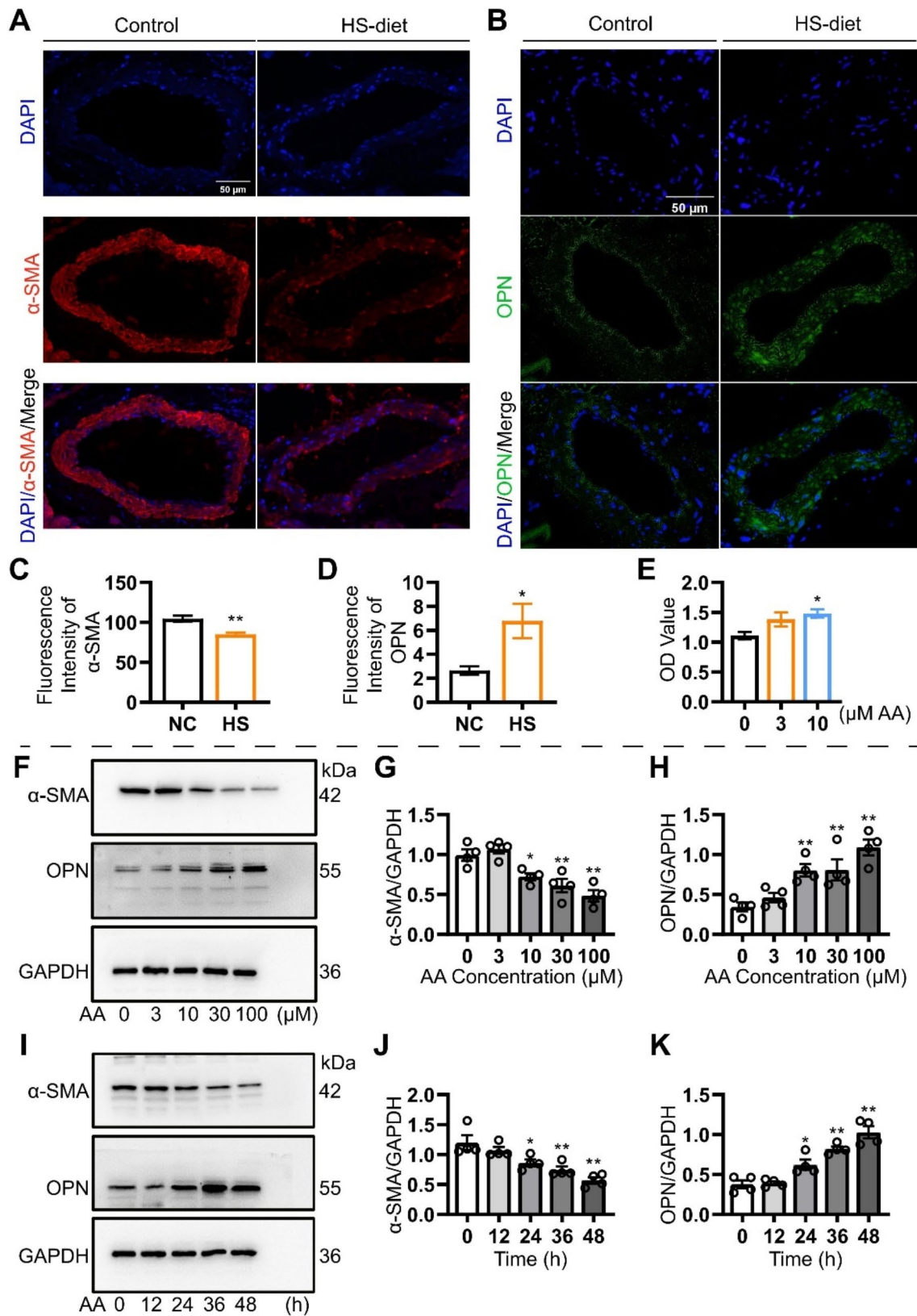


Fig. 2 (See legend on next page.)

(See figure on previous page.)

Fig. 2 A high-salt diet induces coronary artery phenotypic switch. Immunofluorescence detection of **(A)** the vasoconstrictive marker α -SMA ($n=4$), **(B)** the vasodilation marker OPN ($n=4$), and **(C&D)** analysis of fluorescence intensity. The values are presented as the means \pm SEMs, with $n=4$. $*P<0.05$ vs. the normal controls, $**P<0.01$ vs. the normal controls. **(E)** The proliferative capacity of CASMCs was increased by treatment with 10 μ M AA. Representative summary data of the OD values of CASMCs treated with solvent (CON), 3 μ M AA, or 10 μ M AA. **(F)** Representative western blot analysis of α -SMA and OPN protein levels in the CASMCs treated with different concentrations of AA for 24 h. Quantitative analysis of **(G)** α -SMA and **(H)** OPN protein levels in the CASMCs treated with different concentrations of AA for 24 h. The values are presented as the means \pm SEMs, with $n=4$. $*P<0.05$ vs. 0 h, 0 μ M; $**P<0.01$ vs. 0 h, 0 μ M. **(I)** Representative western blot analysis of α -SMA and OPN protein levels in the CASMCs treated with AA (10 μ M) for various durations (0, 12, 24, 36, 48 h). Quantitative analysis of **(J)** α -SMA and **(K)** OPN protein levels in the CASMCs treated with AA (10 μ M) for various durations (0, 12, 24, 36, 48 h). The values are presented as the means \pm SEMs, with $n=4$. $*P<0.05$ vs. 0 h, $**P<0.01$ vs. 0 h. Abbreviations: α -SMA, α -smooth muscle actin; OPN, osteopontin; CASMCs, coronary artery smooth muscle cells; AA, arachidonic acid; OD, optical density; CON, control; SEM, standard error of the mean

Arachidonic acid treatment attenuates agonist-induced vasoconstriction in coronary arteries

The impact of AA on coronary vasoconstriction was investigated. After the coronary arteries were incubated with AA (10 μ M, 24 h), no significant changes in 60 mM K^+ -induced contraction were observed (Fig. 4A). However, upon incubation with AA (10 μ M, 24 h), the contractility of coronary arteries induced by U46619 or $CaCl_2$ decreased. The summary data revealed a decrease in the U46619-induced concentration-dependent contractile responses and $CaCl_2$ -induced concentration-dependent contractile responses (Fig. 4B&C). The data are presented as the means \pm SEMs ($n=6$), $*P<0.05$, versus the normal control. On the basis of these findings, it can be inferred that elevated levels of AA induce coronary artery remodeling and impair vasoconstrictive tension.

Induction of endoplasmic reticulum stress via arachidonic acid metabolism through cyclooxygenase-2

To determine whether AA promotes coronary artery remodeling via COX-2-mediated activation of ERS (Fig. 5A), CASMCs were treated with AA (10 μ M for 24 h) and an additional ERS inhibitor, 4-PBA, in AA-treated cells for 24 h. The immunofluorescence results (Fig. 5B&C) demonstrated that AA treatment significantly increased OPN expression in CASMCs. However, the addition of 4-PBA abolished this increase, further confirming the critical role of ERS in the phenotypic transition of coronary arteries to the proliferative state. Subsequent western blot analysis (Fig. 5D&E) revealed that, compared with the normal controls, the AA-treated CASMCs presented increased expression of ERS markers (GRP78, IRE1 α , p-IRE1 α , and XBP1s). Additionally, the expression of RUNX2, a transcription factor essential for osteoblast differentiation and chondrocyte maturation, as well as its target gene OPN, was increased in the AA-treated CASMCs. Notably, the addition of 4-PBA significantly reduced the expression of ERS-related proteins and RUNX2/OPN. These results demonstrate that ERS inhibition alleviates AA-induced phenotypic transformation in CASMCs. To further investigate the molecular pathways linking AA metabolism and the ERS response, CASMCs were coincubated with the COX-2 inhibitor NS-398 (10 μ M) in the presence of AA. NS-398 is a

cell-permeable compound specifically designed to inhibit COX-2 activity. In this study, incubating CASMCs with appropriate concentrations of AA resulted in an increase in the expression of ERS markers, including GRP78, IRE1 α , p-IRE1 α , and XBP1s. Notably, the expression of the aforementioned ERS markers significantly decreased in response to treatment with NS-398 (Fig. 5F&G). These findings indicate that AA can activate the ERS response through COX-2 catalysis, which can be effectively blocked by NS-398. Collectively, these findings demonstrate that the IRE1 α -XBP1 pathway of the ERS response is regulated by AA/COX-2 and plays a crucial role in the phenotypic transformation of CASMCs.

Discussion

An HS diet is an important dietary risk factor for death, particularly cardiovascular disease-related deaths [22]. This study also suggested that an HS diet induces myocardial ischemia and increases susceptibility to myocardial infarction. A recent Mendelian randomization study [23] found a positive link between genetically forecasted plasma phospholipid AA levels and atherosclerosis. To determine whether the HS diet leads to coronary remodeling and whether this effect is associated with AA, AA levels in the serum of rats fed the HS diet were measured. AA levels were significantly greater in the HS diet-fed rats than in those fed a regular diet. Additionally, the expression of the contractile marker α -SMA in coronary arteries decreased, whereas the expression of the synthetic marker OPN increased in the HS diet group. These results indicate that a HS diet elevates AA levels and induces phenotypic changes in the coronary arteries.

AA is one of the most widely distributed polyunsaturated fatty acids in vivo [24, 25]. The cyclooxygenase (COX) pathway represents one of its primary metabolic routes. Research has consistently demonstrated that the ratio of serum eicosapentaenoic acid (EPA) to AA and higher levels of linoleic acid in serum and tissues are associated with the incidence of cardiovascular events [26, 27]. AA is derived from linoleic acid, and previous studies have shown that in accordance with the precursor/product relationship between linoleic acid and AA, their relative amounts are negatively correlated [28]. This study revealed that an HS diet increases serum AA

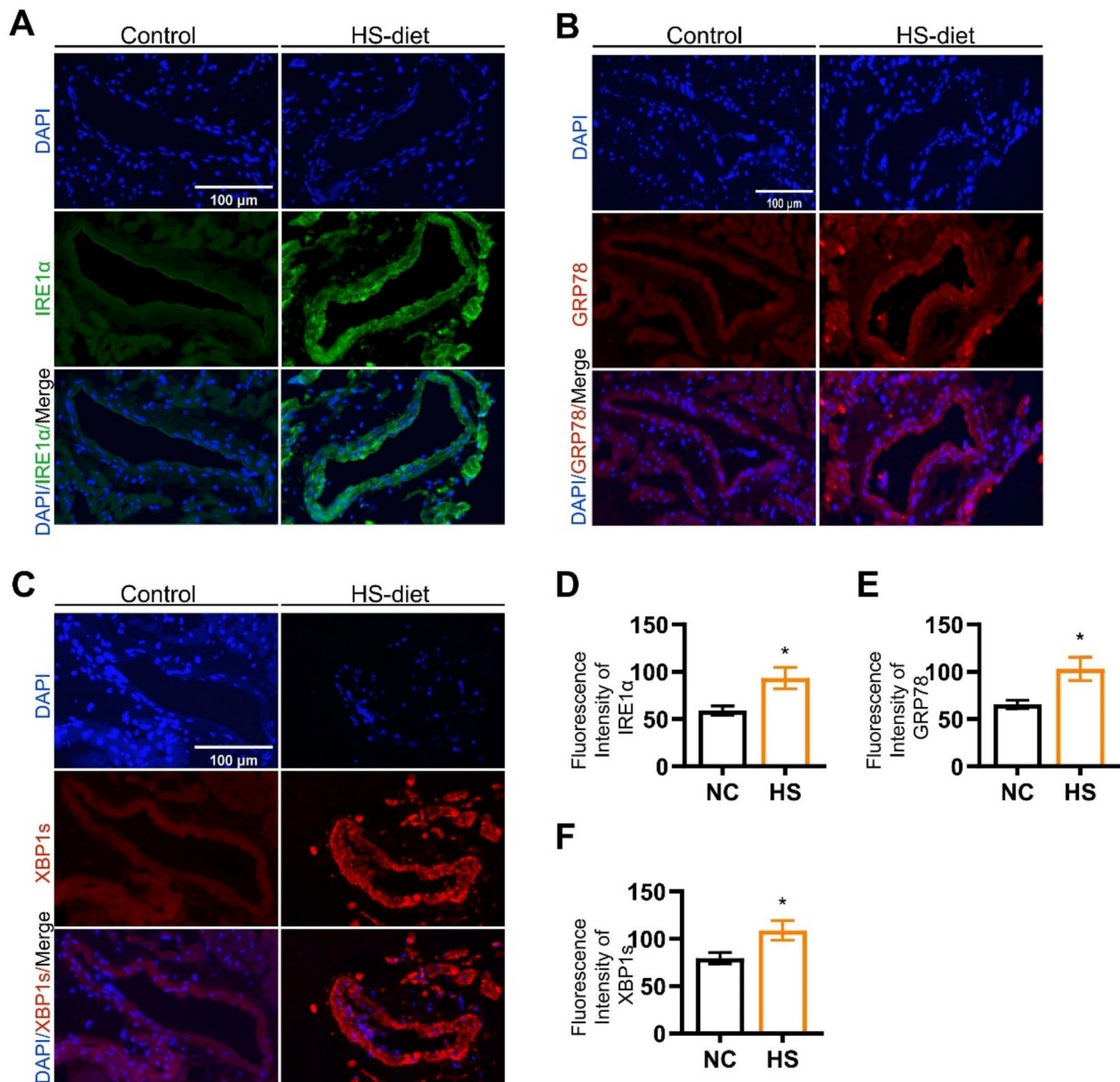


Fig. 3 A high-salt diet increased the expression of endoplasmic reticulum stress-related proteins in coronary arteries. Representative fluorescence intensity of (A) Ire1 α , (B) GRP78 and (C) XBP1s protein signaling in the coronary arteries of the rats fed a high-salt diet compared with those in the normal control group. Quantitative analysis of (D) the Ire1 α , (E) GRP78 and (F) XBP1s protein levels. The data are presented as the means \pm SEMs, with $n=3$. Statistical significance is indicated as * P < 0.05 compared with the normal control group. Abbreviations: Ire1, inositol-requiring enzyme 1; GRP78, glucose-regulated protein 78; XBP1, X-box binding protein-1; SEM, standard error of the mean

levels, which may also suggest that high-salt intake promotes the metabolism of linoleic acid. Further investigations into the relationship between HS diets and linoleic acid metabolism are warranted in future studies. Vascular remodeling plays a crucial role in the occurrence and development of cardiovascular diseases [29, 30]. The transformation of VSMCs induced by inflammation is a key factor in vascular remodeling [31]. This change underlies numerous vascular growth disorders, such

as hypertension, atherosclerosis, and post-angioplasty restenosis [32]. Therefore, elucidation of the phenotypic transformation of VSMCs and the related mechanisms is highly important for the prevention and treatment of cardiovascular diseases. Currently, the mechanisms involved in vascular phenotypic switching include the RhoA/Rho kinase signaling pathway [33], the Wnt signaling pathway [34], the Notch signaling pathway [35], and the TGF- β signaling pathway [36]. Additionally, free AA can be

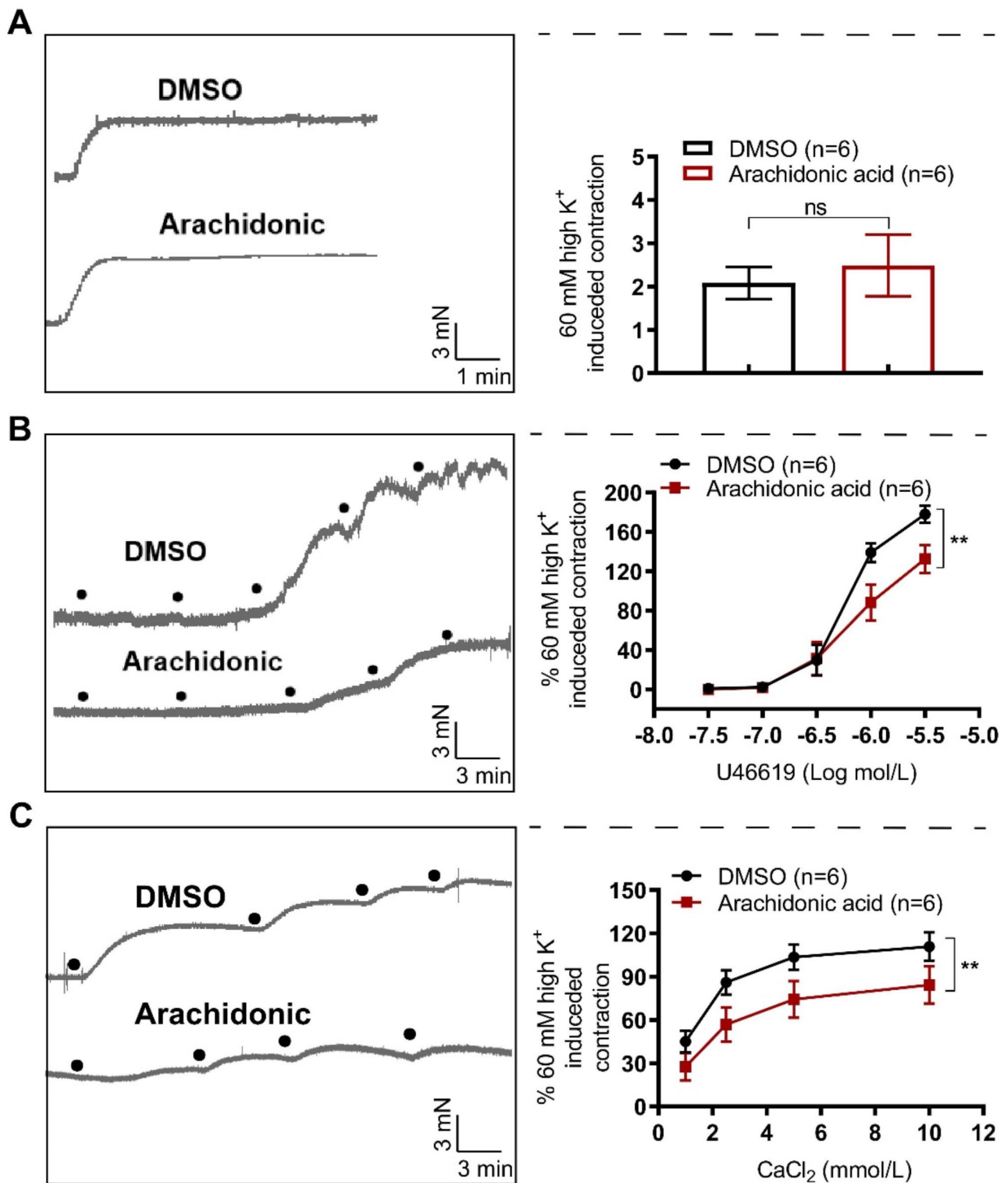


Fig. 4 Arachidonic acid (10 μ M, 24 h) treatment decreased the contractility of coronary arteries in rats. Summary data showing the concentration-dependent contractile responses to **(A)** 60 mM K^+ , **(B)** increasing concentrations of U46619 (0.01, 0.03, 0.1, 0.3, and 1 μ M), and **(C)** CaCl₂ (1, 2.5, 5, and 10 mmol/L) after incubation with AA. The data are presented as the means \pm SEMs, with $n=6$. Statistical significance is indicated as * $P < 0.05$ and ** $P < 0.01$ compared with the normal control group. Abbreviations: U46619, 9, 11-dideoxy-11a, 9a-epoxymetha-noprostaglandin; SEM, standard error of the mean

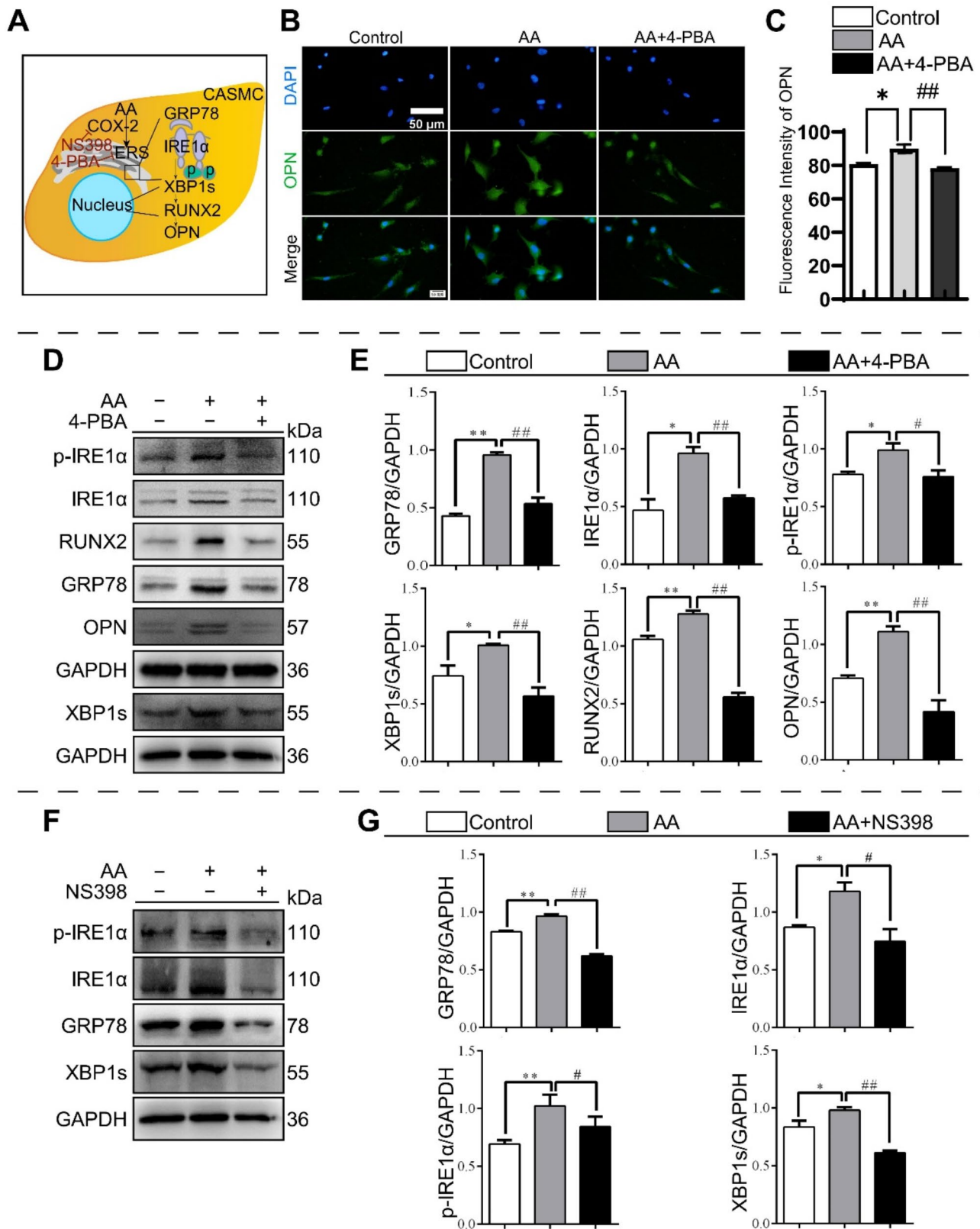


Fig. 5 (See legend on next page.)

(See figure on previous page.)

Fig. 5 Inhibition of cyclooxygenase-2 or endoplasmic reticulum stress improves phenotypic transformation. **(A)** Schematic diagram of molecular studies in coronary smooth muscle cells. **(B)** Immunofluorescence image showing the intensity of OPN in CASMCs incubated with AA (10 μ M, 24 h) or AA (10 μ M, 24 h) + an ERS inhibitor (4-PBA) (1 mM, 24 h) ($n=3$) and **(C)** analysis of fluorescence intensity. The values are presented as the means \pm SEMs, with $n=3$. * $P<0.05$ AA vs. the normal controls, ** $P<0.01$ AA vs. AA+4-PBA. **(D)** Representative western blot and **(E)** quantitative analysis of GRP78, IRE1 α , p-IRE1 α , XBP1s, RUNX2 and OPN protein levels in CASMCs. The values are presented as the means \pm SEMs, with $n=4$. Statistical significance is indicated as * $P<0.05$, ** $P<0.01$ vs. the control group; # $P<0.05$, ## $P<0.01$ vs. the AA (10 μ M, 24 h) group. **(F)** Representative western blot and **(G)** analysis showing the protein levels of the ERS markers GRP78, IRE1 α , p-IRE1 α and XBP1s in the CASMCs incubated with solvent alone, AA (10 μ M, 24 h), or AA (10 μ M, 24 h) + COX-2 inhibitor (NS-398) (10 μ M, 24 h). The values are presented as the means \pm SEMs, with $n=4$. Statistical significance is indicated as * $P<0.05$, ** $P<0.01$ vs. the control group; # $P<0.05$, ## $P<0.01$ vs. the AA (10 μ M, 24 h) group. Abbreviations: OPN, osteopontin; CASMCs, coronary artery smooth muscle cells; AA, arachidonic acid; ERS, endoplasmic reticulum stress; 4-PBA, 4-phenylbutyric acid; GRP78, glucose-regulated protein 78; Ire1, inositol requiring enzyme 1; XBP1, X-box binding protein-1; RUNX2, runt-related transcription factor 2; SEM, standard error of the mean

metabolized by either COX or LOX enzymes, leading to the generation of proinflammatory compounds. Research has demonstrated that AA, along with its inflammatory derivatives, plays a role in regulating the proliferation and apoptosis of vascular smooth muscle cells [37, 38]. However, whether AA induces phenotypic switching in CASMCs is still unclear. In this study, the expression of the specific contraction marker α -SMA decreased after incubation with AA, whereas the synthetic marker OPN increased, indicating a phenotypic switch of CASMCs. Moreover, the coronary contract tension decreased after treatment with AA. On the basis of these findings, it was hypothesized that AA could induce a phenotypic switch in CASMCs, leading to coronary vascular remodeling and a weakening of coronary constriction tension. Thus, an investigation was conducted to explore the underlying mechanisms of this phenomenon.

The AA-COX-2 metabolic pathway plays an important role in cardiovascular diseases. Previous reports [39–41] suggest that the detrimental effects of AA and ERS on the vascular system are associated with apoptosis, calcification, inflammation, and oxidative stress mechanisms. Evidence suggests a potential link between AA and ERS; for example, COX-2 was reported to convert AA to PGE2 when cells were exposed to harmful stimuli. The ERS sensor IRE1 α is closely associated with the expression of COX-2 [42]. The inhibition of PGE2 has been shown to alleviate ERS-mediated apoptosis in osteoarthritis [17]; additionally, the AA-CYP450 pathway induces an ERS response in hepatocytes [16]. However, the specific molecular signaling pathway linking AA and ERS in CASMCs remains unclear. This study revealed that, in HS diet-fed rats, while AA levels were elevated, COX-2 expression in coronary arteries was increased, and the ERS marker proteins Grp78, Ire1 α , p-Ire1 α , and Xbp1s were significantly upregulated after AA incubation. Notably, this upregulation was blocked by the COX-2 inhibitor NS398, suggesting that AA induces an ERS response in CASMCs through the COX-2 pathway. Several studies have shown that the AA-COX2 metabolic pathway typically induces an increase in PGE2 expression, a process closely associated with thrombosis, vascular remodeling, and ischemic heart disease [43, 44], however, this study

did not further verify metabolites of arachidonic acid, including PGE2, and future studies should measure the levels of its metabolites to confirm their involvement in this process. ERS has emerged as a prominent area of research in recent years [1]. Chronic ERS has been implicated in various diseases, including diabetes [45], neurodegenerative diseases [46], shock, and pulmonary fibrosis [47]. Zhao Guizhen et al. reported that the ERS signaling molecule XBP1u directly influences the phenotypic transformation of VSMCs by acting on FOXO4 [48]. Bai, Xiao-Jun et al. demonstrated that ERS increases the expression of RUNX2 in VSMCs, thereby promoting VSMC calcification [49]. This study provides data supporting the role of ERS in promoting coronary artery phenotypic transformation via the XBP1s-RUNX2-OPN axis, leading to remodeling.

OPN is a glycosylated protein that is abundant in the extracellular matrix and has been implicated in various vascular remodeling diseases. OPN is involved in vascular remodeling in conditions such as pulmonary arterial hypertension (PAH) [33]. Furthermore, factors such as high glucose and oxidized LDL can stimulate OPN expression in VSMCs, contributing to the development of atherosclerotic vascular diseases. Increased expression of OPN has been associated with vascular calcification, migration, or proliferation [34–36, 50]. OPN functions downstream of RUNX2, influencing the production of the extracellular matrix. The overexpression of RUNX2 leads to the activation of Osterix, which initiates the expression of bone matrix proteins, including OPN. Moreover, ERS has been shown to increase RUNX2 expression in VSMCs [51]. However, it remains unclear whether AA regulates OPN expression to affect the phenotypic switching of CASMCs. In this study, AA activated the IRE1 α -XBP1s axis of ERS, leading to increased expression of RUNX2. This elevated expression of RUNX2 subsequently promotes OPN protein production, triggering the osteogenic transformation of CASMCs and contributing to their phenotypic changes. Importantly, this mechanism was interrupted by the application of 4-PBA, highlighting its potential therapeutic importance. This research revealed that AA initiates

the phenotypic switch of CASMCs through the IRE1 α -XBP1-RUNX2-OPN pathway following COX-2 catalysis.

Study strengths and limitations

This study focused on the effects of AA on the phenotypic switching of CASMCs. The results revealed several important findings. First, HS diet-fed rats presented ischemic changes in the myocardium and increased susceptibility to myocardial infarction. Furthermore, elevated serum AA levels play a role in coronary artery remodeling. In addition, AA actively facilitates the phenotypic transition of CASMCs via the COX-2 metabolic pathway, mediating ERS responses and engaging downstream signaling pathways involving IRE1 α -XBP1-RUNX2-OPN. Targeted inhibition of key molecules such as COX-2 and ERS effectively alleviated coronary remodeling. These findings increase the understanding of how AA influences the phenotypic switch of CASMCs, shedding light on potential therapeutic targets for cardiovascular diseases associated with excessive AA-derived ERS.

The phenotypic switch of vascular smooth muscle cells is a critical pathological and physiological characteristic that has crucial implications for vascular diseases. In this study, α -SMA and OPN, key markers of phenotypic transition, were specifically highlighted and analyzed. Nevertheless, it is important to note that phenotype switching is a multifaceted process encompassing various stages, and the existing research in this area remains relatively limited, thus warranting further investigation. The *in vitro* effects of AA exposure on CASMCs may reflect potential mechanisms underlying coronary artery remodeling in the context of HS diet-induced increases in serum AA levels. However, the direct link between AA and coronary artery remodeling remains to be confirmed. Future studies should employ more targeted approaches, such as *in vivo* AA supplementation or the treatment of rats with COX-2 inhibitors during an HS diet, to further investigate the direct relationship between high-salt intake and coronary artery AA metabolism.

Conclusions

This study suggests that AA stimulates the phenotypic switch of CASMCs through the ERS-RUNX2-OPN pathway. The identification of AA and RUNX2 as novel therapeutic targets could guide the development of drugs or interventions aimed at modulating these molecules, with the goal of halting or even reversing vascular damage, such as hypertension, atherosclerosis, and heart failure, in patients on high-salt diets.

List of Abbreviations

AA	arachidonic acid
ACh	acetylcholine
α -SMA	α -smooth muscle actin
BiP	binding immunoglobulin protein

CASMCs	coronary artery smooth muscle cells
COX-2	cyclooxygenase-2
CYP450	cytochrome P450
EPA	eicosapentaenoic acid
ERSERS	endoplasmic reticulum stress
FOXO4	Forkhead box O4
GRP78	glucose-regulated protein 78
IRE1	inositol requiring enzyme 1
LOX	lipoygenase
OPN	osteopontin
PAH	pulmonary arterial hypertension
4-PBA	4-phenylbutyric acid
PGE2	prostaglandin E2
RUNX2	runt-related transcription factor 2
TGF- β	transforming growth factor- β
TXA2	thromboxane A2
U46619	9, 11-dideoxy-11a, 9a-epoxymetha-noprostaglandin
XBP1	X-box binding protein-1

Acknowledgements

The authors thank the Comprehensive Experiment Center of Basic Medical Sciences and the Center for Scientific Research of Anhui Medical University for valuable support of this work.

Author contributions

Z.J. and R.Z. were responsible for the experimental design. Z.J. and R.Z. were involved in manuscript writing and revision. Z.J., J.W., F.L., H.W. and P.Z. conducted the experiments and analyzed the data. R.Z. and B.S. supervised the project. All the authors contributed to the article and approved the final manuscript.

Funding

This study was supported by the Natural Science Foundation of China (Grant No. 81970446).

Data availability

No datasets were generated or analysed during the current study.

Declarations

Ethics approval and consent to participate

Not applicable.

Consent for publication

Not applicable.

Competing interests

The authors declare no competing interests.

Received: 3 December 2024 / Accepted: 4 February 2025

Published online: 11 February 2025

References

1. Ponte-Negretti CI, Wyss FS, Piskorz D, Santos RD, Villar R, Lorenzatti A, Lopez-Jaramillo P, Toth PP, Amaro AJJ, Rodrigo AK, et al. Latin American Consensus on management of residual cardiometabolic risk. A consensus paper prepared by the Latin American Academy for the Study of Lipids and cardiometabolic risk (ALALIP) endorsed by the Inter-american Society of Cardiology (IASC), the International Atherosclerosis Society (IAS), and the pan-american college of endothelium (PACE). *Arch Cardiol Mex.* 2022;92:99–112.
2. Sonnweber T, Pizzini A, Nairz M, Weiss G, Tancevski I. Arachidonic Acid metabolites in Cardiovascular and Metabolic diseases. *Int J Mol Sci* 2018; 19.
3. Zhang C, He M, Ni L, He K, Su K, Deng Y, Li Y, Xia H. The role of Arachidonic Acid Metabolism in Myocardial Ischemia-Reperfusion Injury. *Cell Biochem Biophys.* 2020;78:255–65.
4. Huang H, Al-Shabraway M, Wang MH. Cyclooxygenase- and cytochrome P450-derived eicosanoids in stroke. *Prostaglandins Other Lipid Mediat.* 2016;122:45–53.

5. Papageorgiou N, Zacharia E, Briasoulis A, Charakida M, Tousoulis D. Celecoxib for the treatment of atherosclerosis. *Expert Opin Investig Drugs*. 2016;25:619–33.
6. Simon LS. Role and regulation of cyclooxygenase-2 during inflammation. *Am J Med*. 1999;106:S37–42.
7. Sun HJ, Ren XS, Xiong XQ, Chen YZ, Zhao MX, Wang JJ, Zhou YB, Han Y, Chen Q, Li YH, et al. NLRP3 inflammasome activation contributes to VSMC phenotypic transformation and proliferation in hypertension. *Cell Death Dis*. 2017;8:e3074.
8. Lu QB, Wan MY, Wang PY, Zhang CX, Xu DY, Liao X, Sun HJ. Chicoric acid prevents PDGF-BB-induced VSMC dedifferentiation, proliferation and migration by suppressing ROS/NFκB/mTOR/P70S6K signaling cascade. *Redox Biol*. 2018;14:656–68.
9. Lu QB, Wang HP, Tang ZH, Cheng H, Du Q, Wang YB, Feng WB, Li KX, Cai WW, Qiu LY, Sun HJ. Nesfatin-1 functions as a switch for phenotype transformation and proliferation of VSMCs in hypertensive vascular remodeling. *Biochim Biophys Acta Mol Basis Dis*. 2018;1864:2154–68.
10. Lao KH, Zeng L, Xu Q. Endothelial and smooth muscle cell transformation in atherosclerosis. *Curr Opin Lipidol*. 2015;26:449–56.
11. Zhou JJ, Li H, Qian YL, Quan RL, Chen XX, Li L, Li Y, Wang PH, Meng XM, Jing XL, He JG. Nestin represents a potential marker of pulmonary vascular remodeling in pulmonary arterial hypertension associated with congenital heart disease. *J Mol Cell Cardiol*. 2020;149:41–53.
12. Wu X, Lu Q. Expression and significance of alpha-SMA and PCNA in the vascular adventitia of balloon-injured rat aorta. *Exp Ther Med*. 2013;5:1671–6.
13. Wang X, Li H, Zhang Y, Liu Q, Sun X, He X, Yang Q, Yuan P, Zhou X. Suppression of miR-4463 promotes phenotypic switching in VSMCs treated with Ox-LDL. *Cell Tissue Res*. 2021;383:1155–65.
14. Banerjee D, Mazumder S, Kumar Sinha A. Involvement of nitric oxide on Calcium mobilization and arachidonic acid pathway activation during platelet aggregation with different aggregating agonists. *Int J Biomed Sci*. 2016;12:25–35.
15. Oakes SA, Papa FR. The role of endoplasmic reticulum stress in human pathology. *Annu Rev Pathol*. 2015;10:173–94.
16. Park EC, Kim SI, Hong Y, Hwang JW, Cho GS, Cha HN, Han JK, Yun CH, Park SY, Jang IS, et al. Inhibition of CYP4A reduces hepatic endoplasmic reticulum stress and features of diabetes in mice. *Gastroenterology*. 2014;147:860–9.
17. Eo SH, Kim SJ. Rosmarinic acid induces rabbit articular chondrocyte differentiation by decreases matrix metalloproteinase-13 and inflammation by upregulating cyclooxygenase-2 expression. *J Biomed Sci*. 2017;24:75.
18. Kwan HY, Shen B, Ma X, Kwok YC, Huang Y, Man YB, Yu S, Yao X. TRPC1 associates with BK(ca) channel to form a signal complex in vascular smooth muscle cells. *Circ Res*. 2009;104:670–8.
19. Shen B, Cheng KT, Leung YK, Kwok YC, Kwan HY, Wong CO, Chen ZY, Huang Y, Yao X. Epinephrine-induced Ca²⁺ and influx in vascular endothelial cells is mediated by CNGA2 channels. *J Mol Cell Cardiol*. 2008;45:437–45.
20. Hu Y, Li W, Cheng X, Yang H, She ZG, Cai J, Li H, Zhang XJ. Emerging roles and therapeutic applications of Arachidonic Acid pathways in Cardiometabolic diseases. *Circ Res*. 2024;135:222–60.
21. Zhao D, Li J, Xue C, Feng K, Liu L, Zeng P, Wang X, Chen Y, Li L, Zhang Z, et al. TL1A inhibits atherosclerosis in apoe-deficient mice by regulating the phenotype of vascular smooth muscle cells. *J Biol Chem*. 2020;295:16314–27.
22. Collaborators GBDD. Health effects of dietary risks in 195 countries, 1990–2017: a systematic analysis for the global burden of Disease Study 2017. *Lancet*. 2019;393:1958–72.
23. Zhang T, Zhao JV, Schooling CM. The associations of plasma phospholipid arachidonic acid with cardiovascular diseases: a mendelian randomization study. *EBioMedicine*. 2021;63:103189.
24. Wang T, Fu X, Chen Q, Patra JK, Wang D, Wang Z, Gai Z. Arachidonic acid metabolism and kidney inflammation. *Int J Mol Sci*. 2019;20.
25. Innes JK, Calder PC. Omega-6 fatty acids and inflammation. *Prostaglandins Leukot Essent Fat Acids*. 2018;132:41–8.
26. Niwa K, Tanaka A, Funakubo H, Otsuka S, Yoshioka N, Kudo N, Tobe A, Sakakibara K, Miki Y, Kataoka T, et al. The influence of eicosapentaenoic acid to arachidonic acid ratio on Long-Term Cardiovascular events following percutaneous coronary intervention. *Intern Med*. 2021;60:3865–71.
27. Marklund M, Wu JHY, Imamura F, Del Gobbo LC, Fretts A, de Goede J, Shi P, Tintle N, Wennberg M, Aslibekyan S, et al. Biomarkers of Dietary Omega-6 fatty acids and Incident Cardiovascular Disease and Mortality. *Circulation*. 2019;139:2422–36.
28. Hostmark AT, Haug A. Percentage oleic acid is inversely related to percentage arachidonic acid in total lipids of rat serum. *Lipids Health Dis*. 2013;12.
29. Liu H, Xiong W, Luo Y, Chen H, He Y, Cao Y, Dong S. Adipokine Chemerin Stimulates Progression of Atherosclerosis in ApoE(-/-) Mice. *Biomed Res Int*. 2019;2019:7157865.
30. Montezano AC, Tsiropoulou S, Dulak-Lis M, Harvey A, Camargo Lde L, Touyz RM. Redox signaling, Nox5 and vascular remodeling in hypertension. *Curr Opin Nephrol Hypertens*. 2015;24:425–33.
31. Aiyar N, Disa J, Ao Z, Ju H, Nerurkar S, Willette RN, Macphee CH, Johns DG, Douglas SA. Lysophosphatidylcholine induces inflammatory activation of human coronary artery smooth muscle cells. *Mol Cell Biochem*. 2007;295:113–20.
32. Shi J, Yang Y, Cheng A, Xu G, He F. Metabolism of vascular smooth muscle cells in vascular diseases. *Am J Physiol Heart Circ Physiol*. 2020;319:H613–31.
33. Saker M, Lipskaia L, Marcos E, Abid S, Parpaleix A, Houssaini A, Validire P, Girard P, Noureddine H, Boyer L, et al. Osteopontin, a key Mediator expressed by senescent pulmonary vascular cells in Pulmonary Hypertension. *Arterioscler Thromb Vasc Biol*. 2016;36:1879–90.
34. Wolak T. Osteopontin - a multi-modal marker and mediator in atherosclerotic vascular disease. *Atherosclerosis*. 2014;236:327–37.
35. Mazzali M, Kipari T, Ophascharoensuk V, Wesson JA, Johnson R, Hughes J. Osteopontin—a molecule for all seasons. *QJM*. 2002;95:3–13.
36. Li T, Ni L, Liu X, Wang Z, Liu C. High glucose induces the expression of osteopontin in blood vessels in vitro and in vivo. *Biochem Biophys Res Commun*. 2016;480:201–7.
37. Kalyan Krishna S, Parmentier JH, Malik KU. Arachidonic acid-derived oxidation products initiate apoptosis in vascular smooth muscle cells. *Prostaglandins Other Lipid Mediat*. 2002;70:13–29.
38. Anderson KM, Roshak A, Winkler JD, McCord M, Marshall LA. Cytosolic 85-kDa phospholipase A2-mediated release of arachidonic acid is critical for proliferation of vascular smooth muscle cells. *J Biol Chem*. 1997;272:30504–11.
39. Pilane CM, LaBelle EF. Arachidonic acid release by cPLA2 may be causally related to NO-induced apoptosis in vascular smooth muscle cells. *J Cell Physiol*. 2002;191:191–7.
40. Tao J, Zhu W, Li Y, Xin P, Li J, Liu M, Li J, Redington AN, Wei M. Apelin-13 protects the heart against ischemia-reperfusion injury through inhibition of ER-dependent apoptotic pathways in a time-dependent fashion. *Am J Physiol Heart Circ Physiol*. 2011;301:H1471–1486.
41. Myoishi M, Hao H, Minamino T, Watanabe K, Nishihira K, Hatakeyama K, Asada Y, Okada K, Ishibashi-Ueda H, Gabbiani G, et al. Increased endoplasmic reticulum stress in atherosclerotic plaques associated with acute coronary syndrome. *Circulation*. 2007;116:1226–33.
42. Chopra S, Giovanelli P, Alvarado-Vazquez PA, Alonso S, Song M, Sandoval TA, Chae CS, Tan C, Fonseca MM, Gutierrez S et al. IRE1α-XBP1 signaling in leukocytes controls prostaglandin biosynthesis and pain. *Science*. 2019;365.
43. Zhu L, Zhang Y, Guo Z, Wang M. Cardiovascular Biology of prostanoids and Drug Discovery. *Arterioscler Thromb Vasc Biol*. 2020;40:1454–63.
44. Song K, Duan Q, Ren J, Yi J, Yu H, Che H, Yang C, Wang X, Li Q. Targeted metabolomics combined with network pharmacology to reveal the protective role of luteolin in pulmonary arterial hypertension. *Food Funct*. 2022;13:10695–709.
45. Szpigel A, Hainault I, Carlier A, Venticlef N, Batto AF, Hajduch E, Bernard C, Ktorza A, Gautier JF, Ferre P, et al. Lipid environment induces ER stress, TXNIP expression and inflammation in immune cells of individuals with type 2 diabetes. *Diabetologia*. 2018;61:399–412.
46. Hetz C, Saxena S. ER stress and the unfolded protein response in neurodegeneration. *Nat Rev Neurol*. 2017;13:477–91.
47. Burman A, Tanjore H, Blackwell TS. Endoplasmic reticulum stress in pulmonary fibrosis. *Matrix Biol*. 2018;68–69:355–65.
48. Zhao G, Fu Y, Cai Z, Yu F, Gong Z, Dai R, Hu Y, Zeng L, Xu Q, Kong W. Unspliced XBP1 confers VSMC Homeostasis and prevents aortic aneurysm formation via FoxO4 Interaction. *Circ Res*. 2017;121:1331–45.
49. Bai XJ, Liu Y, Gao SS, Zhang WP. [Inhibitory mechanism of icariin against oxidative stress-induced calcification in aortic vascular smooth muscle cells]. *Zhongguo Zhong Yao Za Zhi*. 2021;46:4497–503.
50. Liu J, Ren Y, Kang L, Zhang L. Oxidized low-density lipoprotein increases the proliferation and migration of human coronary artery smooth muscle cells through the upregulation of osteopontin. *Int J Mol Med*. 2014;33:1341–7.

51. Nakahara T, Sato H, Shimizu T, Tanaka T, Matsui H, Kawai-Kowase K, Sato M, Iso T, Arai M, Kurabayashi M. Fibroblast growth factor-2 induces osteogenic differentiation through a Runx2 activation in vascular smooth muscle cells. *Biochem Biophys Res Commun*. 2010;394:243–8.

Publisher's note

Springer Nature remains neutral with regard to jurisdictional claims in published maps and institutional affiliations.